Communication

Investigation of Austenitization in Low Carbon Microalloyed Steel During Continuous Heating

KAVITHA GUNABALAPANDIAN, SANTIGOPAL SAMANTA, RAVI RANJAN, and SHIV BRAT SINGH

Dilatation associated with the formation of austenite from ferrite–pearlite was calculated from equilibrium phase fraction and composition. Linear thermal expansion coefficient of ferrite required for the calculation was determined by iteration of dilatation data. A good match was obtained between the calculated and experimental dilatation curves. The calculated dilatation data were used to identify the stages of austenite formation: pearlite dissolution followed by ferrite to austenite transformation which is gradual at first before becoming rapid.

DOI: 10.1007/s11661-017-4014-0

Austenitization is one of the most important processing steps and significantly influences the final mechanical properties of a given steel. The austenitization process in general depends on the composition, initial microstructure, and processing parameters like heating rate, austenitization temperature, soaking time, *etc*.[1–4] The formation of austenite from a mixture of pearlite and ferrite can broadly be divided into two stages.[2–9] At first, pearlite begins to transform into austenite at Ac_1 and it continues up to Ac_θ. This is followed by proeutectoid ferrite to austenite transformation which is completed at Ac_3. As discussed later, the second stage, *i.e*., ferrite to austenite transformation, can further be divided into two sub-stages. The corresponding equilibrium temperatures are known as Ae_1, Ae_θ, and Ae_3, respectively. Depending on the heating rate, there can be an overlap between these stages of austenite formation.[3] In the present work, studies using a dilatometer were conducted to understand the different stages of austenite formation in a low carbon microalloyed steel during heating at different rates. In addition, the experimental dilatation curve at the slowest heating rate studied was compared with the calculated dilatation curve using the equilibrium phase transformation and lattice parameter data.

Dilatometry is one of the experimental techniques that is frequently used to understand the phase transformation behavior in steels.[2–12] The dilatometer utilizes the fact that the change in length of a material is influenced by the temperature and phase transformation. An increase in the temperature generally leads to expansion of the material while phase transformation may result in an overall contraction or expansion depending on the phases involved. Any deviation from linear thermal expansion (or contraction during cooling) indicates transformation.

The composition of the as-received hot-rolled steel plate used in the current study is given in Table I. Cylindrical samples, with 4 mm diameter and 10 mm length, for dilatometer tests were prepared using a wire EDM machine. All the experiments were performed in vacuum (5×10^{-4} mbar) or in inert atmosphere (during cooling cycle) in Bähr 805 A/D dilatometer having a resolution of 5 μm/5 °C. The temperature change was measured and controlled by a Pt and Pt-10 wt pct Rh thermocouple spot welded on the surface of sample, and argon gas was used to control the cooling rates.

The samples were heated to 1173 K (900 °C) at different heating rates (0.05, 0.5, and 5 K s^{-1}), followed by soaking at that temperature for 300 seconds and cooling to room temperature (Figure 1(a)). In another case, heating of the sample was interrupted at the Ac_θ temperature and the sample was quenched to room temperature to understand the microstructure development (Figure 1(b)). This was done for the slowest heating rate of 0.05 K s^{-1} and the cooling from the intermediate temperature was sufficiently high to prevent any ferrite or pearlite transformation.

The critical transformation temperatures (Ac_1, Ac_θ, and Ac_3) were determined by analyzing the changes in the dilatation curve following two different approaches, namely, the "*Tangent*" and "*First Differential*" methods.

Samples for microstructural characterization were obtained by cutting the samples along the transverse direction near the thermocouple welds. These samples were then mechanically ground and polished following the standard procedure and finally etched with 2 pct nital solution. Microstructure of the samples was examined with the help of LEICA®DM6000M optical microscope.

The as-received hot-rolled sample consisted of ferrite (volume fraction: 0.86 ± 0.03) and pearlite (volume fraction: 0.14 ± 0.03) (Figure 2).

The relative change in length and its first differential with respect to temperature for the heating rate of

KAVITHA GUNABALAPANDIAN, RAVI RANJAN, and SHIV BRAT SINGH are with the Department of Metallurgical and Materials Engineering, Indian Institute of Technology Kharagpur, Kharagpur 721 302, India. Contact e-mail: ravimetalbitjsr@gmail.com SANTIGOPAL SAMANTA is with the Research and Development (R&D) Division, Tata Steel Ltd., Jamshedpur 831 001, India.

Manuscript submitted October 26, 2016.
Article published online February 17, 2017

Table I. Composition of the Investigated Steel (All in Weight Percent)

C	Mn	Si	Nb	S	P	Fe
0.09	1.39	0.25	0.058	0.012	0.021	bal.

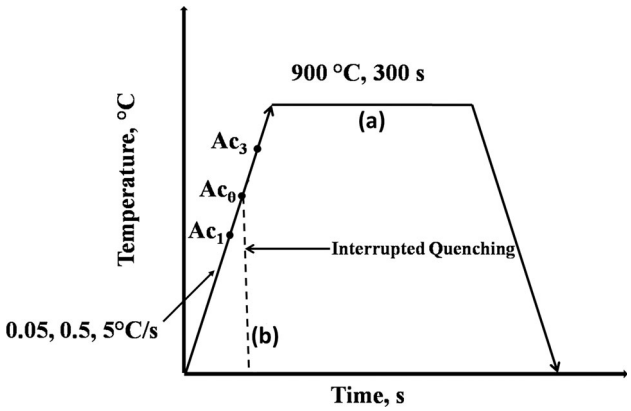

Fig. 1—Schematic heat treatment diagram: (*a*) Austenitization treatment with varying heating rate and (*b*) Quenching treatment.

0.05 K s^{-1} are shown in Figure 3 where the transformation starts and the end temperatures are indicated as Ac_1 and Ac_3, respectively.

The dilatation curve shown in Figure 3 can be divided into 3 segments in the transformation region based on the points of deviation identified as points 1, 2, 3, and 4. These segments represent: (i) a contraction between points 1 to 2, (ii) a small expansion between points 2 to 3, and (iii) a continuous contraction between points 3 to 4, the contraction in this segment is gradual at first and then it becomes quite rapid. Similar results have been reported in earlier studies where these stages are evident in the reported dilatation curves.[2,4,6–9]

To understand the changes in the dilatation behavior in the individual stages, it is important to consider the factors which contributes to the dilatation curve. The dilatation curve is basically a reflection of the contribution from thermal expansion and phase transformations involved.[3] Assuming that the change in dimensions of the sample due to transformation is isotropic, it can be shown that the relative change in length ($\Delta L/L_o$) associated with transformation of ferrite and cementite to austenite (including thermal expansion of the phases) at a given temperature T can be expressed as[6,9,12,15]:

$$\frac{\Delta L}{L_0} = \frac{1}{3}\frac{\left[2f_\alpha' a_\alpha'^3 + \frac{1}{3}f_\theta' a_\theta' b_\theta' c_\theta' + f_\gamma' a_\gamma'^3\right] - \left[2f_\alpha a_\alpha^3 + \frac{1}{3}f_\theta a_\theta b_\theta c_\theta\right]}{\left[2f_\alpha a_\alpha^3 + \frac{1}{3}f_\theta a_\theta b_\theta c_\theta\right]}, \quad [1]$$

where ΔL is the total change in length of the sample up to a given temperature T and L_o is the initial length of the sample at room temperature. a_α and $a_\theta, b_\theta, c_\theta$ are the lattice parameters of ferrite and cementite at room temperature, respectively, while, a_α', a_γ' and $a_\theta', b_\theta', c_\theta'$ are the lattice parameters of ferrite, austenite, and cementite at temperature T, respectively. Similarly, f_α and f_θ are the initial volume fractions of ferrite and cementite at the room temperature, respectively, while, f_α', f_γ', and f_θ' are the volume fractions of ferrite, austenite, and cementite at temperature T, respectively.

Equation [1] suggests that the calculation of dilatation curve requires a knowledge of the changes in the fraction of the phases with temperature and the corresponding lattice parameters. Lattice parameter in turn depends on the composition of the phase and temperature. For this, the amount and the composition of the phases involved were first calculated using Thermo-Calc software (Figure 4(a)). Variations in the lattice parameter of the phases with composition and temperature were calculated using the equations given in Table II. The thermal expansion coefficients of the individual phases were estimated from the experimental dilatation data as described below to calculate the change in lattice parameter with temperature.

The linear regions of the dilatation curve in Figure 3, *i.e.*, the regions below point 1 (representing Ac_1) and above point 4 (representing Ac_3), represent the zones of thermal expansion only with no phase transformation. Therefore, the thermal expansion coefficient of the phases can be estimated simply from the slope of the curve in the respective thermal expansion regions. However, it should be noted that the initial microstructure of the samples subjected to dilatometry in the present work was ferrite and pearlite (Figure 2) and the slope of the dilatation curve obtained from data before point 1 (Ac_1) in Figure 3 corresponds to thermal expansion of a phase mixture of ferrite and cementite. The slope of this part of the dilatation curve cannot therefore be taken to be equal to the thermal expansion coefficient of ferrite or cementite and used directly in Eq. [1]. Therefore, a procedure involving iteration was used to extract the linear thermal expansion coefficient value of ferrite (β_α) from the experimental dilatation curve using the known linear thermal expansion coefficient value of cementite (β_θ) given in Table II.[15,16] Iteration was performed on the dilatation data below point 1 (Ac_1) using Eq. [1] and setting f_γ' to zero and taking $f_\alpha' = f_\alpha$ and $f_\theta' = f_\theta$ since there is no transformation in this region. The objective of iteration was to minimize the difference between the calculated and experimental dilatation data in the region below point 1. The linear thermal expansion coefficient of austenite was also obtained from a similar exercise on the dilatation data above point 4 (Ac_3) in Figure 3. In both the cases, correlation coefficient (r^2) values were close to 1. The values of β_α and β_γ estimated by this approach were $1.543 \times 10^{-5}\,K^{-1}$ and $2.071 \times 10^{-5}\,K^{-1}$, respectively. The complete dilatation curve was thereafter calculated using Eq. [1] for the equilibrium phase fractions and composition (Figure 4(a)). The calculated dilatation

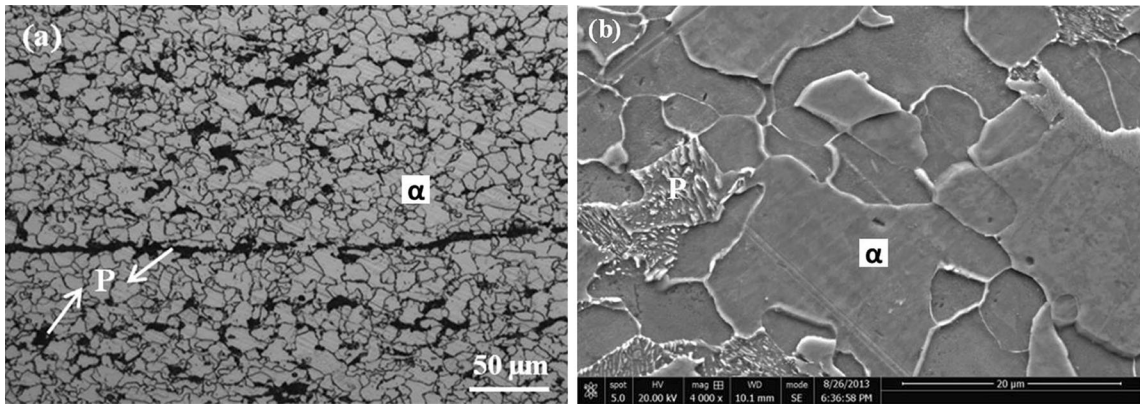

Fig. 2—(*a*) Optical and (*b*) SEM micrograph of the as-received steel; etched with 2 pct nital. α: ferrite, P: pearlite.

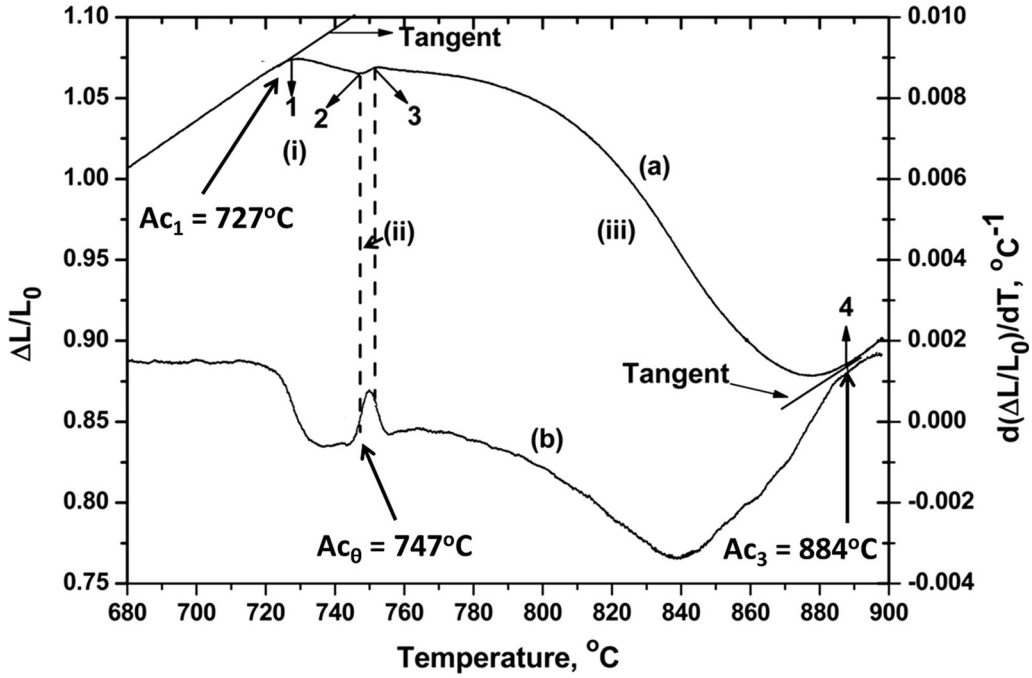

Fig. 3—Curve (*a*) represents the dilatation curve of the sample during continuous heating up to 1173 K (900 °C) at the rate of 0.05 K s^{-1} and curve (*b*) is the first derivative $d(\Delta L/L_0)/dT$ plotted as a function of temperature.

curve thus obtained is shown in Figure 4(b). The experimental dilatation curve for the slowest heating rate of 0.05 K s^{-1} is also shown in Figure 4(b) for comparison.

The stages of austenite formation in the experimental and calculated dilatation curves are marked as points 1 to 4 and 1e to 4e, respectively in Figure 4. Similar to the experimental dilatation curve, the calculated dilatation curve shows linear thermal expansion till point 1e (Ae_1), after which it begins to deviate from linearity. The equilibrium austenite transformation start temperature (Ae_1) is 954 K (681 °C). The equilibrium phase fraction plot (Figure 4(a)) and the corresponding calculated dilatation curve (Figure 4(b)) suggest that the first contraction from point 1e to 2e [Ae_θ = 964 K (691 °C)] is due to pearlite dissolution and it agrees quite well with the experimental dilatation curve (points 1 to 2). However, the actual temperature at which the experimental curve deviates from linearity at point 1 is higher than the equilibrium value, because of a finite heating rate employed, so that, the difference in temperature between points '1e' and '1' represents the degree of superheating at which the dissolution of pearlite actually begins at a heating rate of 0.05 K s^{-1}. After pearlite gets transformed to austenite, the proeutectoid ferrite begins to transform to austenite at point 2e. This transformation is gradual at first between points 2e and 3e and then it picks up after point 3e as is evident from Figure 4(a). The calculated dilatation curve in Figure 4(b) reflects this behavior. Since the transformation of ferrite to austenite is relatively gradual between points 2e and 3e, the contraction due to the transformation is very small, but the thermal expansion in this temperature range is larger than the contraction due to

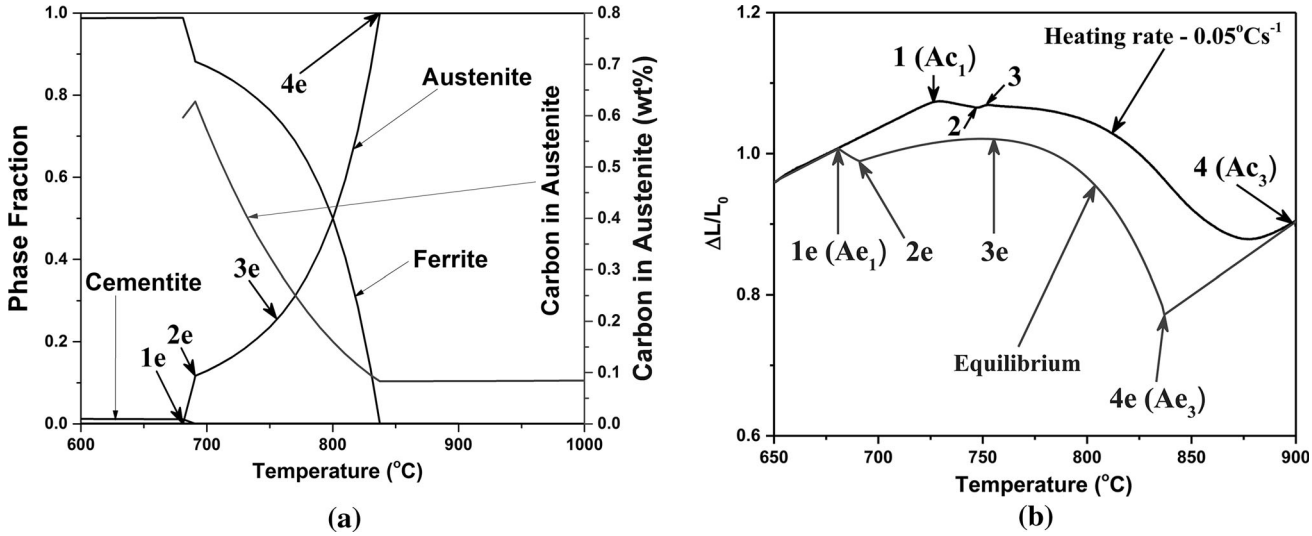

Fig. 4—(*a*) Equilibrium volume fraction of the phases and the corresponding wt pct of C in austenite as a function of temperature and (*b*) Experimental (heating rate: 0.05 K s^{-1}) and calculated dilatation curves of the steel.

Table II. Lattice Parameter of Ferrite, Austenite, and Cementite as a Function of Composition and Temperature

Phases	Equations for Lattice Parameter Calculation	References
Ferrite (α) and Austenite (γ)	$a'_p = a_p[1 + \beta_p(T - 298)]$; p is ferrite ($\alpha$) or austenite ($\gamma$) $a_\alpha = 2.8664 + 0.0006\,[\mathrm{Mn}] - 0.0003\,[\mathrm{Si}] - 0.0010\,[\mathrm{P}]$ $a_\gamma = 3.5770 + 0.0065\,[\mathrm{C}] + 0.0010\,[\mathrm{Mn}] + 0.0079\,[\mathrm{Nb}]$ Here [X] represents the concentration of element X in at. pct, β_p is the linear thermal expansion coefficient of the phase identified by the subscript p, T is in Kelvin, and a_p in Å	13,14
Cementite (θ)	$a'_\theta = a_\theta[1 + \beta_\theta(T - 298)]$; $b'_\theta = b_\theta[1 + \beta_\theta(T - 298)]$; $c'_\theta = c_\theta[1 + \beta_\theta(T - 298)]$; $\beta_\theta = 6.0 \times 10^{-6} + 3.0 \times 10^{-9}(T - 273) + 1.0 \times 10^{-11}(T - 273)^2\ \mathrm{K}^{-1}$	15,16

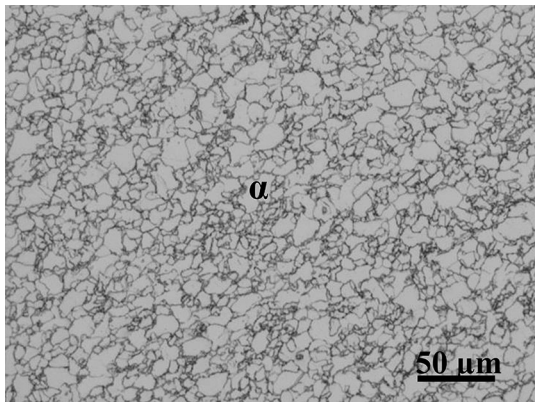

Fig. 5—Microstructure of the sample quenched from pearlite dissolution temperature Ac_θ [1020 K (747 °C)]; etched with 2 pct nital. α—ferrite.

the transformation resulting in a small net expansion in the calculated dilatation curve between points 2e and 3e. The transformation then becomes rapid after point 3e resulting in large and rapid contraction between points 3e and 4e. This explains the small expansion observed in the experimental dilatation curve between points 2 and 3 followed by a gradual and then rapid contraction between points 3 and 4. Finally, the ferrite to austenite transformation gets completed at point 4e on the calculated phase fraction plot and the dilatation curve, the corresponding point on the experimental curve is marked as point 4; these points represent Ae_3 and Ac_3 temperatures, respectively. Once the austenite formation is complete at point 4e, the curve becomes linear with temperature to reflect thermal expansion of austenite. There is thus a close match between the calculated and the experimental dilatation curves showing different stages of austenite formation, *i.e.*, pearlite dissolution and ferrite to austenite transformation.

To further confirm that point 2 [1020 K (747 °C)] in Figure 3 actually corresponds to the end of pearlite dissolution (Ac_θ), heating (at 0.05 K s^{-1}) was interrupted at this temperature and the sample was quenched to room temperature. The microstructure of this sample in Figure 5 clearly shows complete disappearance of pearlite, confirming that point 2, where the initial contraction ends, represents the Ac_θ temperature.

The transformation start and finish temperatures are other parameters that are important for the design of heat treatment cycle. As stated earlier, these

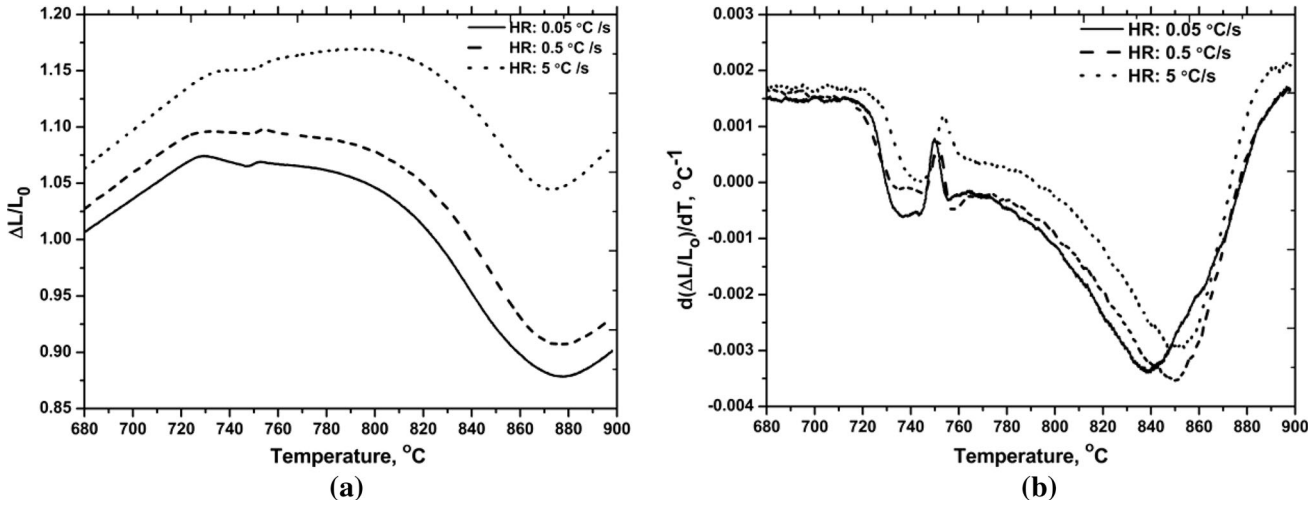

Fig. 6—(*a*) Dilatation curves at constant heating rates of 0.05, 0.5, and 5 K s^{-1} and (*b*) $d(\Delta L/L_0)/dT$ *vs* temperature for the three heating rates.

Table III. Critical Transformation Temperatures of the Steel Sample for Three Heating Rates

Heating rate (K s^{-1})	Ac_1 [K (°C)]	Ac_θ [K (°C)]	Ac_3 [K (°C)]
0.05	1000 (727)	1020 (747)	1157 (884)
0.5	1001 (728)	1021 (748)	1160 (887)
5	1005 (732)	1022 (749)	1163 (890)

temperatures can be obtained from the dilatation curve by (a) Tangent method, and (b) First differential method. In the tangent method, the temperature at which the dilatation curve deviates from (linear) thermal expansion or contraction is estimated to indicate the transformation start and finish temperatures. While this method is generally used for quick estimation of the transformation temperature, a more accurate and sharp indication of these temperatures can be obtained by the first differential method where the first derivative of the relative change in length with respect to temperature (T) $[d(\Delta L/L_0)/dT]$ is plotted against temperature. The first derivative of the dilatation curve and the estimated pearlite dissolution temperature for the hearing rate of 0.05 K s^{-1} are shown in Figure 3.

The effect of heating rate on the dilatation curves and the corresponding first derivative of the dilatation curves are shown in Figure 6. The critical transformation temperatures obtained from these curves are given in Table III. Figure 6(a) shows that the contraction associated with pearlite dissolution between points 1 and 2 becomes more gradual with increasing heating rates. In addition, the critical temperatures increased slightly with the increase in the heating rate from the lowest (0.05 K s^{-1}) to the highest (5 K s^{-1}) heating rate studied in this work (Table III). Similar results have been reported in other studies in literature.[2,4,8,9,12] For example, the critical temperatures were found to increase with heating rate in the range of heating rates studied (0.05 to 10 K s^{-1}) in 0.11 C-1.5 Mn (wt pct) Nb-microalloyed steel similar to the one investigated in the present work.[2]

In summary, low C microalloyed steel sample was continuously heated up to 1173 K (900 °C) in a dilatometer to study the dilatation associated with austenitization. The dilatation curve indicates that the formation of austenite in this steel takes place in stages (Figure 3). In order to understand these stages and interpret the experimental dilatation curve, a theoretical dilatation curve was calculated considering the equilibrium phase fractions of ferrite, cementite, and austenite as a function of temperature, their composition, lattice parameters, and the volume change associated with the formation of austenite from ferrite and/or cementite (Figure 4). The calculated dilatation curve matched very well with the experimental dilatation curve. The results indicate that the contraction in the dilatation curve observed between points 1 and 2 in Figure 4(b) is due to the transformation of pearlite into austenite. Interrupted quenching tests confirm this (Figure 5). Pearlite dissolution is followed by transformation of ferrite into austenite with a concomitant decrease in the carbon content of austenite that forms (Figure 4(b)). The transformation is gradual at first (between points 2 and 3 in Figure 4(b)) which may show up as a small expansion in the dilatation curve during heating because the thermal expansion due to heating is more than the contraction due to transformation. The transformation

then becomes rapid resulting in a sharp contraction (points 3 to 4 in Figure 4(b)) before eventually tapering off when the austenite formation nears completion.

The authors acknowledge partial financial support from Ministry of Steel and Department of Science and Technology, Government of India.

REFERENCES

1. G. Krauss: *Steels: Processing, Structure and Performance*, ASM International, Materials Park, 2005.
2. D.S. Martín, T. de Cock, A. García-Junceda, F.G. Caballero, C. Capdevila, and C.G. de Andrés: *Mater. Sci. Technol.*, 2008, vol. 24, pp. 266–72.
3. V.I. Savran, Y.V. Leeuwen, D.N. Hanlon, C. Kwakernaak, W.G. Sloof, and J. Sietsma: *Metall. Mater. Trans. A*, 2007, vol. 38, pp. 946–55.
4. F.L.G. Oliveira, M.S. Andrade, and A.B. Cota: *Mater. Charact.*, 2007, vol. 58, pp. 256–61.
5. G.R. Speich, V.A. Demarest, and R.L. Miller: *Metall. Trans. A*, 1981, vol. 12, pp. 1419–28.
6. C.G. de Andrés, F.G. Caballero, and C. Capdevila: *Scr. Mater.*, 1998, vol. 38, pp. 1835–42.
7. M. Gómez, S.F. Medina, and G. Caruana: *ISIJ Int.*, 2003, vol. 43, pp. 1228–37.
8. D.S. Martín, P.E.J. Rivera-Díaz-del-Castillo, and C. García-de-Andrés: *Scr. Mater.*, 2008, vol. 58, pp. 926–29.
9. F.G. Caballero, C. Capdevila, and C.G. De Andrés: *ISIJ Int.*, 2001, vol. 41, pp. 1093–1102.
10. F.G. Caballero, C. Capdevila, and C.G. de Andrés: *Mater. Sci. Technol.*, 2001, vol. 17, pp. 1114–18.
11. M. Takahashi and H.K.D.H. Bhadeshia: *J. Mater. Sci. Lett.*, 1989, vol. 8, pp. 477–78.
12. C.G. de Andrés, F.G. Caballero, C. Capdevila, and L.F. Alvarez: *Mater. Charact.*, 2002, vol. 48, pp. 101–11.
13. W.C. Leslie: *The Physical Metallurgy of Steels*, 1st ed., Hemisphere Publishing Corporation, New York, 1981.
14. D.J. Dyson and B. Holmes: *J. Iron Steel Inst.*, 1970, vol. 208, pp. 469–74.
15. C.G. de Andrés, F.G. Caballero, C. Capdevila, and H.K.D.H. Bhadeshia: *Scr. Mater.*, 1998, vol. 39, pp. 791–96.
16. H. Stuart and N. Ridley: *J. Iron Steel Inst.*, 1966, vol. 204, pp. 711–17.